

Pressure induced structural phase transitions and metallization of BaF₂

V. Kanchana, G. Vaitheeswaran, M. Rajagopalan*

Department of Physics, Anna University, Chennai 600 025, India

Received 25 October 2002; received in revised form 29 January 2003; accepted 29 January 2003

Abstract

The electronic band structure of BaF₂ was calculated in the fluorite, orthorhombic and the hexagonal phases. The calculations were performed using the tight binding linear muffin tin orbital method (TB-LMTO). The total energies calculated within the atomic sphere approximation (ASA) were used to determine the ground state properties of the system. The calculated equilibrium lattice constants and the bulk modulus are in good agreement with the experimental results. The calculated transition pressure for fluorite→orthorhombic and orthorhombic→hexagonal phases are 2.84 and 12.8 GPa, respectively, which are in good agreement with the experimental results. In addition, BaF₂ is predicted to undergo metallization around 33 GPa. The band structures are plotted in all the three phases and at metallization. The band gap in the three phases are 7.03, 7.16, 3.34 eV, respectively. The calculated density of states at the metallization is around 10.57 states/Ry/F.U. This system is found to be an indirect band gap insulator with the band gap initially increasing with pressure which decreases upon further compression leading to band overlap metallization.

© 2003 Elsevier B.V. All rights reserved.

Keywords: Inorganic materials; Phase transition; High pressure; Electronic band structure

1. Introduction

Under ambient conditions, divalent metal halides AF₂ (A=Ba, Ca, Sr, Pb) generally crystallize in the cubic fluorite structure. Crystals with this structure have been largely studied due to their applications as scintillation detectors and super ionic conductors. In particular BaF₂ is a high-density luminescent material, which is largely used for γ -ray and elementary particle detection [1]. At present BaF₂ crystal array is the state of the art equipment for measuring high-energy γ -ray photons. BaF₂ crystal has an excellent timing property and this property is used to discriminate against neutrons, which are a major source of contamination of high-energy γ -ray spectrum at intermediate energies. As the time resolution of BaF₂ crystals is much better than that of NaI crystal, BaF₂ crystal can discriminate against neutrons using a much shorter time of flight. So BaF₂ crystal array can be placed much closer to the target, thus covering a much larger solid angle [2]. The influence of the hydrostatic pressure on the properties of fluorite compounds has been studied by different techniques. In general, the pressure dependence of the elastic

coefficients, dielectric constant, lattice parameters and Raman spectra suggests the existence of at least, one structural transformation namely an orthorhombic phase at high-pressures. This behaviour was confirmed in CaF₂, SrF₂, BaF₂ and PbF₂ crystals [3–7]. The study of the phase transitions in solids and the interpretation of such transitions in terms of the dynamics of the crystal lattice are of prime importance. A joint experimental and theoretical study of the dynamical and structural properties of lead fluoride (PbF₂) has been carried out by Lorenzana et al. [8]. They reported a transition at about 4 kbar from the cubic (β) to the orthorhombic (α) phase. At approximately 147 Kbar, they observed a transformation from the α phase to the γ phase, which is structurally similar to the orthorhombic α phase. Combined first-principle pair wise simulations and quantum-mechanical ab initio perturbed ion (AIPI) calculations have been extensively performed to determine the static equations of state of the cubic and orthorhombic polymorphs of CaF₂ [9]. X-ray diffraction and theoretical studies of the high-pressure structures and phase transitions in magnesium fluoride has been carried out by Haines et al. [10]. In MgF₂, a second order transition from the tetragonal rutile type to an orthorhombic CaCl₂-type phase is observed at 9.1 GPa, prior to the transformation at close to 14 GPa to the cubic phase, which is found to have a modified fluorite structure of the

*Corresponding author. Tel.: +91-44-235-1265x3153; fax: +91-44-235-2870.

E-mail address: mrajagopalan@lycos.com (M. Rajagopalan).

PdF_2 type. The results of the density functional calculation for MgF_2 yields the following sequence of stable phases: rutile $\rightarrow \alpha\text{PbO}_2 \rightarrow \text{PdF}_2 \rightarrow \alpha\text{PbCl}_2$ and indicate that fluorite-type structure always has a higher energy than PdF_2 -type structure and is never stable for MgF_2 . Molecular dynamics studies on the shock-induced phase transition of a MgF_2 crystal was performed by Nishidate et al. [11]. The post-Cotunnite phase in BaCl_2 , BaBr_2 , and BaI_2 under high pressure was studied by Leger et al. [12], using angle-dispersive powder diffraction method. According to them, these Cotunnite structure compounds ($Pnam$, $Z=4$) at ambient conditions transform to a common monoclinic high-pressure structure between 5 and 15 GPa at room temperature. High-pressure transformation in Cotunnite-type BaCl_2 was found to occur around 21 GPa [13]. Cotunnite structured compounds PbCl_2 , SnCl_2 , BaCl_2 , BaBr_2 were investigated under high pressure by X-ray diffraction and were found to undergo a phase transition to a monoclinic structure between 7 and 16 GPa [14]. Diffuse phase transition studies in cubic fluorite type BaF_2 were performed by Oberchmidt and Catlow [15,16]. Though there are a lot of experimental works available for BaX_2 ($X=\text{F}, \text{Cl}, \text{Br}, \text{I}$), regarding the high-pressure structural phase transitions, there is no theoretical work available to verify the above transition especially by TB-LMTO method. There are many other studies available for these alkaline earth fluorides. Pressure induced colour centers in CaF_2 and BaF_2 was studied by Minomura et al. [17]. Superionicity studies in alkaline earth fluorides CaF_2 , BaF_2 and SrF_2 have been done by Zhon et al. [18] using molecular dynamical simulations. The ionic conductivity studies of fluorite-type compounds (CaF_2 , SrF_2 , BaF_2 , SrCl_2) have been performed at high temperatures by Voronin et al. [19]. The photo acoustic spectra studies on $\text{BaX}_2:\text{Eu}^{2+}$ ($X=\text{F}, \text{Cl}, \text{Br}$) phosphors were carried out by Yugeng [20]. High-pressure X-ray and neutron diffraction studies of BaF_2 were carried out by Leger et al. [7]. They reported a transition from fluorite to orthorhombic phase around 3 GPa. A second crystallographic transition is reported above 12 GPa wherein the high-pressure phase is of Ni_2In type structure. BaF_2 is an indirect band gap insulator with the band gap of the order of 10 eV. Hence it becomes interesting to see whether it undergoes insulator to metal transition at high-pressures in addition to the structural phase transitions reported experimentally. It is also essential to find whether the structural phase transition or the metallization occurs first in this system. Band structure generally serves as a tool to classify materials as metals, semiconductors or insulators. But in the present case there is no band structure available even at ambient conditions. Hence efforts have been to study the structural phase transitions, metallization and the ground state properties of BaF_2 using TB-LMTO method. Band structure is plotted in all the three phases and the density of states is plotted after the metallization of BaF_2 . The rest of the paper is organized as following. Section 2 deals with the

structural aspects of these phases. Section 3 gives the computational details. Results and discussions are elaborated in Section 4. Finally Section 5 gives the conclusion.

2. Crystallographic aspects

BaF_2 at ambient conditions, presents the cubic fluorite structure which consists of three interpenetrating monoatomic f.c.c. sub lattices, one of them occupied by barium and two by fluorine ions [1]. It belongs to the cubic $Fm\bar{3}m$ space group with four molecules per unit cell. In the cubic fluorite phase, the 'Ba' atom is at the position (0, 0, 0) and the 'F' atom is positioned at (0.25, 0.25, 0.25). Under hydrostatic pressure, two-phase transitions are induced in BaF_2 crystals. At about 3 GPa, the fluorite phase transforms into an orthorhombic cotunnite type structure [7]. In the cotunnite type structure with the space group $Pnam$, the 'Ba' atom is at (0.259, 0.112, 0.25), 'F1' is at (0.361, 0.433, 0.25) and 'F2' is at (0.039, 0.320, 0.75). The axial ratios b/a and c/a are minimized at a fixed volume and it is found to be 1.2650 and 0.64, respectively. These minimized values are in fairly good agreement with the experimentally reported values of 1.275 and 0.65. The cation co-ordination number increases from 8 to 9 as we go from fluorite to the cotunnite structure. Under ambient conditions or at high-pressures, over 400 compounds adopt the orthorhombic cotunnite structures [21]. Although the cotunnite structure presents the highest co-ordination observed in AX_2 compounds at ambient conditions, several compounds transform into a highly co-coordinated phase at high-pressures. In the case of BaX_2 ($X=\text{Cl}, \text{Br}, \text{I}$), the new phase has a monoclinic structure ($P112_1/a$, $Z=8$) where the metal ion has the ten-fold co-ordination [14,22]. On the other hand BaF_2 follow a different path by transforming into a hexagonal Ni_2In type structure ($P6_3/mmc$) from the cotunnite structure at pressures above 12 GPa [7]. In this structure, the barium co-ordination number increases to 11. In the Ni_2In type structure, the barium and the two fluorine atoms occupy the following positions, (1/3, 2/3, 1/4), (0,0,0), (1/3, 2/3, 3/4), respectively. As the axial ratios are minimized in the orthorhombic phase and were in good agreement with the experimental results, the experimentally reported c/a value is used in this Ni_2In type structure. This structure can also be presented in an orthorhombic description using the space group $Pnam$ and the lattice parameters satisfy the following relation: $a_0 = c_h$, $b_0 = \sqrt{3} a_h$, $c_0 = a_h$. In the present case, calculations are performed based on the Ni_2In type structure with the space group ($P6_3/mmc$).

3. Computational details

To compute the electronic structure and the basic ground state properties of BaF_2 , TB-LMTO (tight binding linear

muffin tin orbital method) has been used [23,24]. von-Barth and Hedin [25] parameterization scheme has been used for the exchange correlation potential within the local density approximation (LDA). The accuracy of the total energies obtained within the density-functional theory, often using LDA, is in many cases sufficient to predict which structure at a given pressure has the lowest free energy [26]. Atomic sphere approximation (ASA) has been used in the present work [27]. In this approximation, the crystal is divided into space filling spheres centered on each of the atomic site. Combined correction terms are also included, which account for the non-spherical shape of the atomic spheres and the truncation of the higher partial waves inside the sphere to minimize the error in the LMTO-method. In the present case, one empty sphere is added in the fluorite type structure and six spheres in the orthorhombic cotunnite type structure. In the Ni_2In type structure no empty spheres are added, as it is a close packed structure. The Wigner–Seitz sphere is chosen in such a way that the sphere boundary potential is minimum and the charge flow is in accordance with the electronegativity criteria. ‘s’, ‘p’ and ‘d’ partial waves are included. The tetrahedron method [28] of the Brillouin zone (k -space) integration has been used to calculate the density of states. The ‘5p’ states of barium and ‘2s’ states of fluorine are treated as the valence states in the present calculation.

4. Results and discussions

4.1. High-pressure phase transitions:

In order to study the structural phase transitions in BaF_2 , the total energies were calculated in a manner similar to our earlier works [29,30] by reducing the volume from $1.05V_0$ to $0.6V_0$, where V_0 is the experimental equilibrium volume. The calculated total energies are fitted to the Birch equation of state [31] to obtain the pressure volume relation. The graph connecting the pressure and the relative volume in all the three phases is shown in Fig. 1. The bulk modulus is also calculated from the P – V relation using the formula:

$$B = -V \frac{dP}{dV} \quad (1)$$

The theoretically calculated lattice constant and the bulk modulus in all the three phases are given in Table 1 and are compared with the available literature [1,6,7]. At a given pressure, a stable structure is one for which enthalpy has its lowest value and the transition pressures are calculated at which the enthalpies for the two phases are equal. The graph connecting the total energies and the relative volume in all the three phases is shown in Fig. 2. From the graph it can be clearly seen that the fluorite phase is the most stable phase. The transition pressures from the fluorite to the orthorhombic phase and then to the hexagonal-

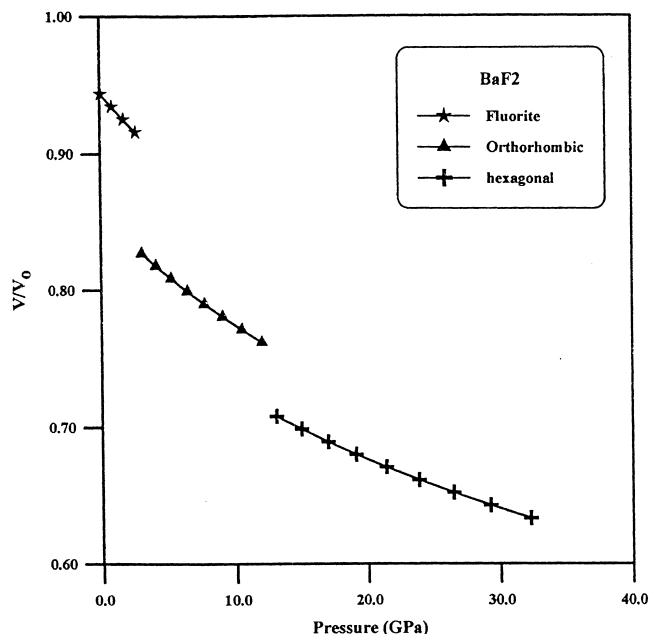


Fig. 1. Calculated pressure volume relation in the fluorite, orthorhombic and hexagonal phases of BaF_2 .

al phase is tabulated in Table 2 along with the volume collapse. The calculated transition pressures compare well with the earlier experimental work [7]. BaF_2 is predicted to undergo insulator to metal transition at about 33 GPa, which is in agreement with the works of [7,32] who have proposed that BaF_2 undergo a reversible metallisation at pressures above 30 GPa. The lattice parameter in the fluorite phase is 11.50 a.u, which agrees well with the experimental value of 11.72 [33]. The calculated value of lattice parameter underestimates the experimental value by 1.89%. There are no experimental results available to compare the lattice parameters at the transition to the orthorhombic and hexagonal phases. The calculated bulk moduli in all the three phases are 79.64, 91.39, 136.21 GPa, respectively. The bulk modulus is overestimated in the fluorite phase by about 38%. The calculated values of bulk modulus of alkaline-earth fluorohalides by Kalpana et al. [34] using the TB-LMTO method deviates from the experimental value by 35%. This error may be due to the inherent limitation of LDA. In addition the ground state properties such as the cohesive energy and the inter-atomic distances in all the three phases are tabulated in Table 1.

4.2. Band structure and density of states

The self-consistent band structure for BaF_2 is obtained at ambient as well as at high-pressures, in order to study the effect of pressure on the band gap. Fig. 3 shows the band structure plots for BaF_2 in the fluorite phase. The lowest lying band arises from the F2s states, which are well separated from the other bands. The bands lying above this arise mainly from the Ba5p like states. The

Table 1
Calculated ground state properties of BaF₂ at ambient and high-pressure

Properties	Fluorite		Orthorhombic		Hexagonal	
	Theory	Exp.	Theory	Exp.	Theory	Exp.
Lattice parameter (a.u)	11.50	11.72 [33]	$a=11.80$ $b=14.93$ $c=7.56$	– – –	$a=7.99$ $c=10.36$	– –
Bulk modulus (GPa)	79.64	57 [7]	91.39	79±10 [7]	136.21	133±16 [7]
Ba–F (a.u)	4.99	–	4.83	–	4.61	–
F–F (a.u)	5.76	–	5.39	–	5.17	–
Band gap (eV)	7.03	9.1 [35]	7.16	–	3.34	–
Cohesive energy (eV)	18.04	–	17.93	–	17.53	–

Relevant experimental data taken from the references given in square brackets.

upper valence bands, which lie close to the Fermi level, are contributed by the 3p states of the fluorine atoms. From Fig. 3 we can see that the top of the valence band occurs at the Z-point. The conduction band arises from the '5d' and '6s' states of the metal atom and the bottom of the band occurs at the Γ point making the compound to be an indirect band gap insulator with a band gap of 7.033 eV. This deviates from the earlier reported value by 22% [35]. This order of error arises due to the use of LDA, which underestimates the zero pressure band gaps by 30–50% [36,37]. The gap is again indirect in the orthorhombic phase with the valence band maximum occurring at U and conduction band minimum occurring at the Γ point and the value is 7.16 eV. Fig. 4 shows the indirect gap in the

orthorhombic phase at the transition. The band gap initially increases with pressure in the fluorite phase and decreases upon further compression in the orthorhombic phase. This is similar to that observed in alkali-earth fluorohalides and many of the II–IV semiconductors [34,38–40]. At the transition to the Ni₂In type structure the gap becomes a direct one at the Γ point, which is around 3.34 eV. As we further compress the F2s states starts moving up towards the Fermi level and the Ba6s and 5d states moves down towards the Fermi level. They lie very close to each other and the gap is much less which is 0.02 eV along the M – Γ direction. At the metallization the Ba '5d' states drops down below the Fermi level and there is an overlap between the F '2p' and Ba '5d' like states and the density of states is found to be around 10.57 states/Ryd/F.U at the Fermi level. The band structure at the metallization is given in Fig. 5.

The density of states is plotted at the metallization in the hexagonal phase. It can be clearly seen from Fig. 6 that the major contribution to the density of states is from the Ba5d and 6s like states. The metallization pressure, band gap values are tabulated in Table 2.

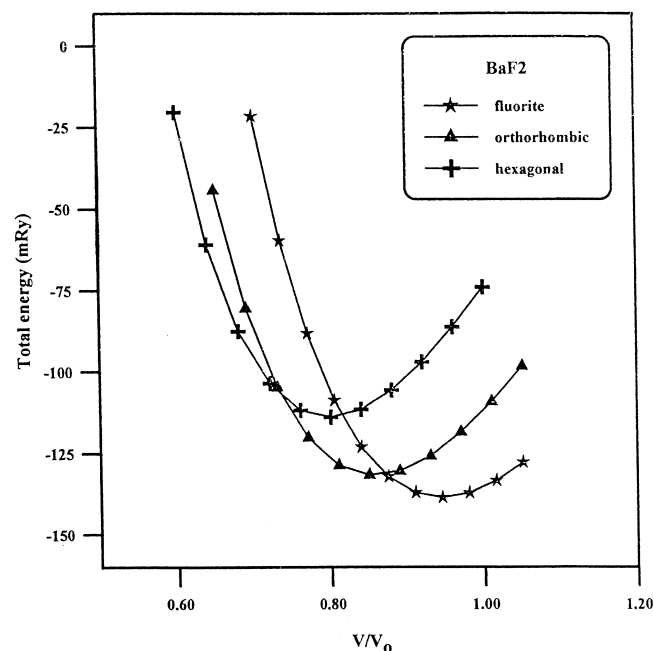


Fig. 2. Calculated total energy (–16659.00+) Ry vs. relative volume in the fluorite, orthorhombic and hexagonal phases of BaF₂.

5. Conclusion

The structural and electronic properties of BaF₂ have been calculated using the TB-LMTO method. From the total energy calculations it can be seen that the fluorite phase is the most stable phase. It is found to undergo a series of structural phase transitions under pressure. The sequence of the structural phase transition is as follows: Fluorite $Fm\bar{3}m \rightarrow$ Orthorhombic ($Pnam$) \rightarrow Hexagonal ($P6_3/mmc$). The transition pressures are 2.84 and 12.8 GPa, respectively, which compares well with the experimental value reported by Leger et al. [7]. BaF₂ is a wide band gap insulator with a band gap of 7.033 eV. Upon compression it is predicted to undergo insulator to metal transition around 33 GPa. The calculated transition pressure, volume collapse and ground state properties agree

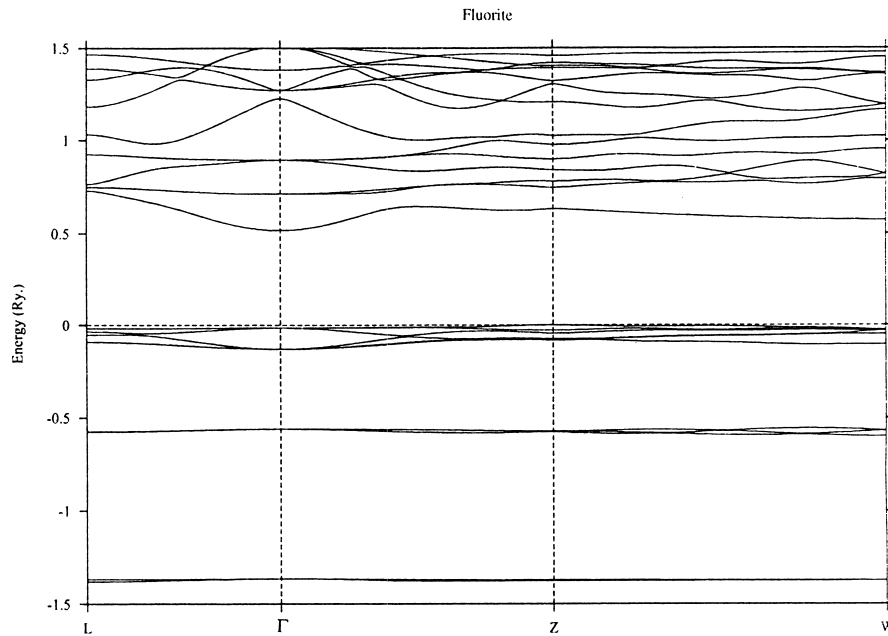


Fig. 3. Band structure of BaF₂ in the fluorite phase.

well with the experimental results. As BaF₂ is predicted to undergo metallization at pressures, which can easily be attained by diamond anvil cell, it could be easily verified experimentally.

The band structure is plotted at ambient as well as at high-pressures. Initially it has an indirect band gap occurring between the ‘p’ like valence band of the anion and

‘sd’ like conduction bands of the metal atom. This calculated value of the band gap underestimates the experimental value by 22% [35]. As stated earlier this error may be due to the usage of LDA [36,37]. Upon compression the band gap initially increases and then decreases on further compression leading to the band overlap metallization. The density of states at the metallisation is found to

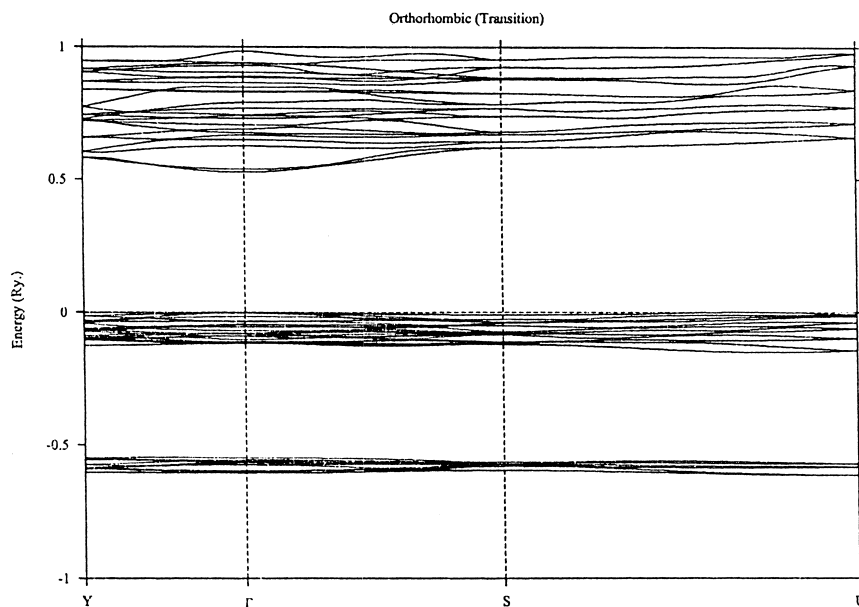


Fig. 4. Band structure of BaF₂ in the orthorhombic phase at the transition.

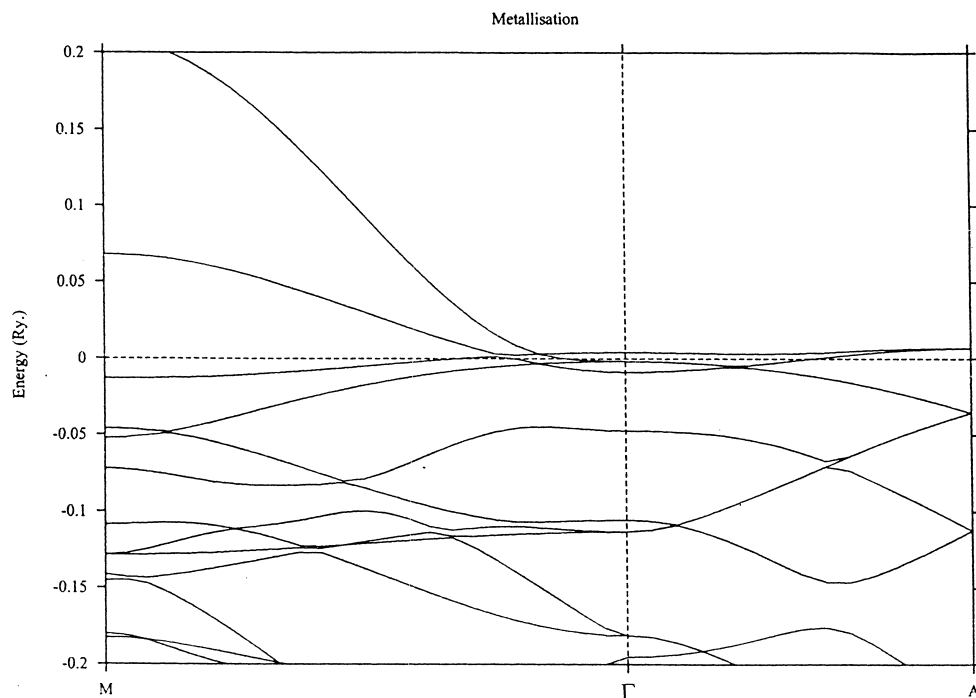


Fig. 5. Band structure of BaF_2 in the hexagonal phase at the metallization.

be around 10.57 States/Ryd/F.U. To our knowledge this is the first band structure calculation reported. Due to the non-availability of the experimental or theoretical results, it is not possible to compare the calculated band-structure

results. The transfer of electrons from the fluorine 'p' like states to the 's' and 'd' like states of barium may be the possible reason for the above-mentioned phenomenon of metallization.

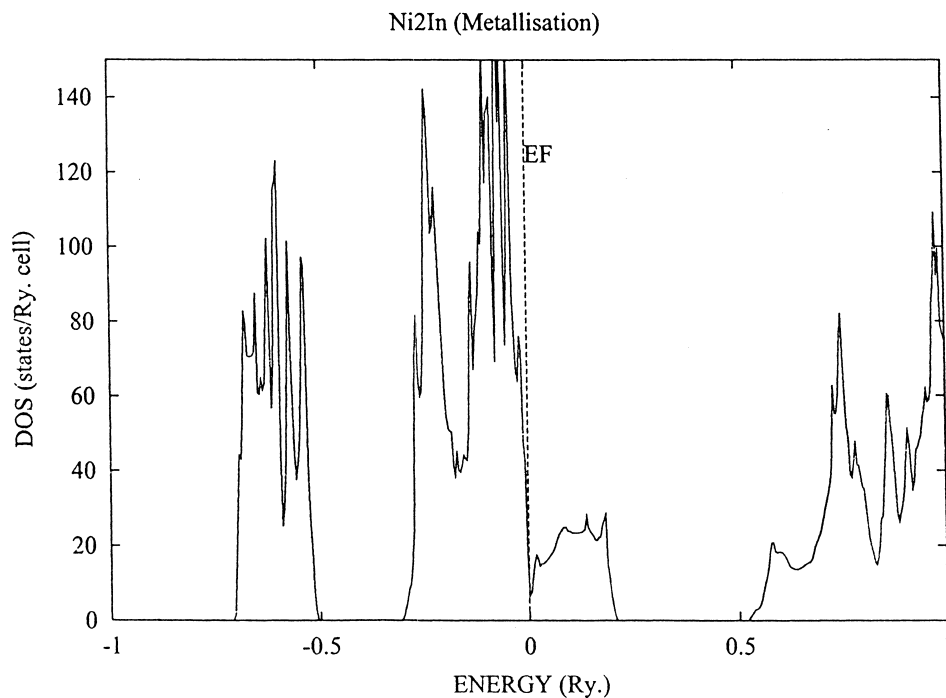


Fig. 6. Density of states of BaF_2 in the hexagonal phase at the metallization.

Table 2
Calculated transition pressure and volume collapse of BaF₂

Transitions	Transition pressure (GPa)		Volume collapse (%)	
	Theory	Experiment	Theory	Experiment
Fluorite→Orthorhombic	2.84	3 [7]	9.28	8.5 [7]
Orthorhombic→Hexagonal	12.8	13 [7]	6.29	–
Metallization	33	–	–	–

Experimental data taken from Ref. [7].

References

- [1] A.P. Ayala, *J. Phys. Condens. Matter* 13 (2001) 11741.
- [2] A. Ray, S.R. Banerjee, P. Das, *Pramana J. Phys.* 57 (2001) 141.
- [3] H.I. Smith, J.H. Chen, *Bull. Am. Phys. Soc.* 11 (1966) 414.
- [4] D.P. Dandekar, J.C. Jamieson, *Trans. Am. Crystallogr. Assoc.* 5 (1969) 1.
- [5] G.A. Samara, *Phys. Rev. B* 2 (1970) 4194.
- [6] G.A. Samara, *Phys. Rev. B* 13 (1976) 4529.
- [7] J.M. Leger, J. Haines, A. Atouf, O. Schuete, S. Hull, *Phys. Rev. B* 52 (1995) 13247.
- [8] H.E. Lorenzana, J.E. Klepeis, M.J. Lipp, W.J. Evans, H.B. Radousky, M. van Schilfhaarde, *Phys. Rev. B* 56 (1997) 543.
- [9] A. Martin Pendas, J.M. Recio, M. Florez, V. Luana, M. Bermijo, *Phys. Rev. B* 49 (1994) 5858.
- [10] J. Haines, J.M. Leger, F. Gorelli, D.D. Klug, J.S. Tse, Z.Q. Li, *Phys. Rev. B* 64 (2001) 134110.
- [11] K. Nishidate, M. Babu, T. Sato, K. Nishikawa, *Phys. Rev. B* 52 (1995) 3170.
- [12] J.M. Leger, J. Haines, A. Atouf, *J. Appl. Crystallogr.* 28 (1995) 416.
- [13] J.M. Leger, A. Atouf, *J. Phys. Condens. Matter* 4 (1992) 357.
- [14] J.M. Leger, J. Haines, A. Atouf, *Phys. Rev. B* 51 (1995) 3902.
- [15] J. Oberschmidt, *Phys. Rev. B* 23 (1991) 5038.
- [16] C.R.A. Catlow et al., *J. Phys. C* 3197 (1978) 1.
- [17] S. Minoiuta, H.G. Drickamer, *J. Chem. Phys.* 34 (1961) 670.
- [18] L.X. Zhou, J.R. Hardy, H.Z. Cao, *Solid State Commun.* 98 (1996) 341.
- [19] B.M. Voronin, S.V. Volkov, *J. Phys. Chem. Solids* 62 (2001) 1349.
- [20] Z. Yugeng, *Phys. Rev. B* 51 (1995) 14849.
- [21] B.G. Hyde, M. O'Keefe, W.M. Lyttle, N.E. Brese, *Phys. Rev. B* 57 (1992) 764.
- [22] J.M. Leger, J. Haines, A. Atouf, *J. Phys. Chem. Solids* 57 (1996) 7.
- [23] O.K. Andersen, *Phys. Rev. B* 12 (1975) 3060.
- [24] H.L. Skriver, *The LMTO Method*, Springer, Heidelberg, 1984.
- [25] U. von Barth, L. Hedin, *J. Phys. C* 5 (1972) 1629.
- [26] N.E. Christensen, D.L. Novikov, R.E. Alonso, C.O. Rodriguez, *Phys. Status Solidi (b)* 211 (1999) 5.
- [27] O.K. Andersen, O. Jepsen, *Phys. Rev. Lett.* 53 (1984) 2871.
- [28] O. Jepsen, O.K. Andersen, *Solid State Commun.* 9 (1971) 1763.
- [29] V. Kanchana, G. Vaitheeswaran, M. Rajagopalan, *J. Alloys Comp.* 352 (2003) 60.
- [30] G. Kalpana, B. Palanivel, M. Rajagopalan, *Phys. Status Solidi (b)* 184 (1994) 153.
- [31] F. Birch, *J. Geophys. Res.* 83 (1978) 1257.
- [32] B.V. Vinogradov, L.F. Vereshchagin, E.N. Yakovlev, Y.A. Timofeev, *Pisma Zh. Tekh. Fiz* 2 (1976) 964, [*Sov. Tech. Phys. Lett.* 2 (1976) 856].
- [33] R.W.G. Wyckoff, 2nd Edition, *Crystal Structures*, Vol. 1, Interscience, New York, 1982.
- [34] G. Kalpana, B. Palanivel, I.B. Shameem Banu, M. Rajagopalan, *Phys. Rev. B* 56 (1997) 3532.
- [35] W.A. Harrison, *Electronic Structure and Properties of Solids*, Freeman, San Francisco, 1980.
- [36] C. Stampfl, C.G. Van de Walle, *Phys. Rev. B* 59 (1998) 5521.
- [37] M. Biagini, *J. Phys. C* 8 (1996) 2233.
- [38] K.J. Chang, S. Froyen, M.L. Cohen, *Solid State Commun.* 50 (1984) 105.
- [39] S. Ves, U. Schwarz, N.E. Christensen, K. Syassen, M. Cardona, *Phys. Rev. B* 42 (1990) 9113.
- [40] A. Mang, K. Reimann, S. Rudennacke, *Solid State Commun.* 94 (1995) 251.